Journal Pre-proof

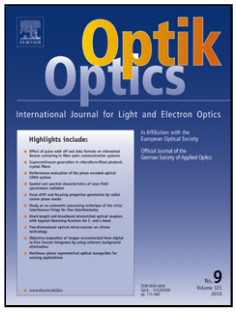

Dynamics of pulse amplification in tapered-waveguide quantum-dot semiconductor optical amplifiers

Aram Fardi, Hamed Baghban, Mohammad Razaghi

PII: S0030-4026(20)30230-8

DOI: https://doi.org/10.1016/j.ijleo.2020.164396

Reference: IJLEO 164396

To appear in: *Optik*

Received Date: 3 January 2020

Accepted Date: 11 February 2020

Please cite this article as: Fardi A, Baghban H, Razaghi M, Dynamics of pulse amplification in tapered-waveguide quantum-dot semiconductor optical amplifiers, *Optik* (2020), doi: https://doi.org/10.1016/j.ijleo.2020.164396

Dynamics of pulse amplification in tapered-waveguide quantum-dot semiconductor optical amplifiers

Aram Fardi[1], Hamed Baghban[2], and Mohammad Razaghi[3]

[1]*Department of Electrical Eng., School of Eng., University of Kurdistan, Sanandaj, Iran*
[2]*Department of Electrical and Computer Engineering, University of Tabriz, Tabriz, Iran*
[3]*Department of Electrical Eng., School of Eng., University of Kurdistan, Sanandaj, Iran*

**Corresponding author: h-baghban@tabrizu.ac.ir*

Abstract

Tapered-waveguide quantum dot semiconductor optical amplifiers (TW-QDSOAs) have been modeled using numerical calculation of the rate and propagation equations in this article and the amplification characteristics and dynamics of pulse propagation in non-tapered QDSOA, linear, and exponential TW-QDSOA structures have been studied and compared in detail. It has been found that TW-QDSOAs apply less distortion to the amplified pulse and have greater optical gain than non-tapered QDSOA. In TW-QDSOAs, the amplified pulse becomes much less broadening and this amount is negligible, therefore the pulse bit rate can be increased. While the amplified pulse in a non-tapered QDSOA is much broadening than the TW-QDSOAs. The carrier density distribution and dependency of the amplifier gain to the output energy for both non-tapered and tapered structures have been studied. The carrier density and gain in non-tapered QDSOA decreases more than TW-QDSOAs, indicating that the tapered amplifiers are saturated at higher input energies. Our obtained results agree well with those previously obtained for conventional tapered amplifiers.

keywords— Quantum dot semiconductor optical amplifier, tapered QDSOA, gain saturation

1. Introduction

During the last decades, semiconductor optical amplifiers (SOAs) play an essential role in optical communication networks [1]. SOAs are multipurpose devices that can be used as an optical detector [2], optical switching element, wavelength converter, logical gate and signal processor in addition to amplification and noise suppression of optical signals [3-8]. While conventional SOAs have different operational weaknesses such as low saturation output power, low optical gain, and low operation bandwidth, quantum-dot semiconductor optical amplifiers (QDSOAs) have promising characteristics due to their low threshold current [9, 10], wide optical bandwidth [11], high thermal stability [12], high bit-rate signal processing [13], and the low impact of carrier heating on the gain and phase recovery [14]. Due to presence of a carrier reservoir in the excited state (ES) and wetting layer (WL), QDSOAs have large saturation output power and also, the optical gain recovery is performed much faster compared with their conventional counterparts based on bulk and quantum well (QW) structure [14, 15].

The sharp decrease in carrier densities as the light intensity increases along the cavity is one of the main disadvantages of a conventional straight or non-tapered cavity. Reducing the carrier density results in an early saturation of the SOAs which limits the power-dependent applications of an amplifier. To solve this problem, a larger cross-sectional area for the active region should be used. A larger active region makes it possible to provide a larger number of carriers, which will increase the saturation output power. The

introduction of tapered-waveguide (TW) structures for the active region in SOAs was an attempt to resolve the aforementioned challenge [16]. In a TW structure, the width of the active region from the input to the output can be increased linearly, exponentially, quadratic, or based on a Gaussian function.

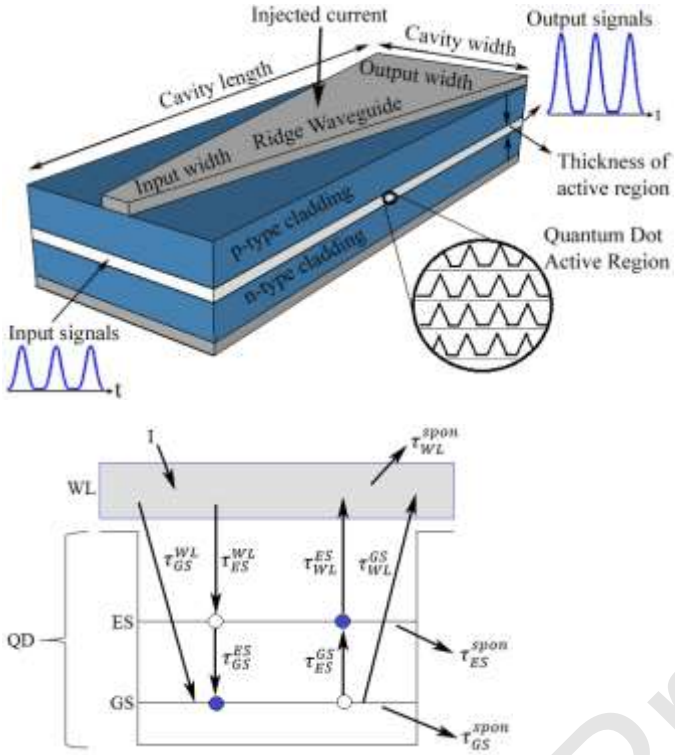

Fig. 1. Schematic illustration of a linear TW-QDSOA with a cross-sectional view of self-assembled quantum dots (upper panel) and the energy band diagram of a QD including the carrier transitions between the energy levels (lower panel).

A TW-SOA provides higher saturation output power and also higher optical gain [17-19]. Therefore, the amplified output pulse is less distorted compared to a conventional non-tapered SOA [20]. The carrier density distribution, pulse amplification along the cavity and the variation of pulse gain with the input pulse energy have been investigated for non-tapered and tapered bulk amplifier structures [20].

Due to the advantages of QDSOAs compared to conventional SOAs and characteristic efficiency of TW structures for the active region of a SOA compared to straight-cavity SOAs, the dynamics and operational characteristics of a TW-QDSOA have been investigated for the first time in this manuscript.

In this study, performance characteristics of a picosecond Gaussian pulse propagation in a non-tapered QDSOA have been analyzed compared with the TW-QDSOAs with both linearly and exponentially-tapered waveguides. Variation of the carrier density, gain saturation, pulse width, and also, the temporal shift in the gain peak along the amplifier cavity have been studied for three structures and the results compared in detail. The provided discussions are organized as follows. The device structure and also the mathematical relations governing the TW-QDSOA are expressed in section 2. Simulation results and discussion are presented in section 3 and finally, a short summary of the obtained results is presented in section 4.

2. Device Structure and Theoretical Background

The schematic illustration of the linear TW-QDSOA structure along with the energy band diagrams of the active region of a QD has been illustrated in Fig. 1. The injected carriers fill the ground state (GS) of QDs and the input signal will be amplified through stimulated emission or processed through optical nonlinearities of the QDs, like cross-phase modulation or cross-gain modulation phenomena. As illustrated in Fig. 1, depending on the design features of a QDSOA, the active region may consist of several QD layers. A barrier material covers the QDs inside the active region and their WL and therefore, the dot layers are isolated. The transition between the GS if the conduction band to GS of the valence band has been assumed to be the optical transition which is stimulated by the input signal. Also, the direct carrier capture from the WL into the GS is neglected due to the large energy separation between the GS and the WL and the fast intra-dot carrier relaxation. The SOA bias current is directly injected into the wetting layer and the theoretical model doe not explicitly include carrier transport phenomena such as drift or diffusion processes.

The rate equations of the QDSOA for the WL, ES, and GS are similar to the model presented in [4, 21]. However, the rate equations in a TW-QDSOA require modification due to the variation of the waveguide width along the cavity. Therefore, the rate equations can be rewritten as follows:

$$\frac{\partial N_W(z,\tau)}{\partial \tau} = \frac{I}{eV} - \frac{N_W(1-h)}{\tau_{W2}} + \frac{\tilde{N}_Q h}{\tau_{2W}} - \frac{N_W}{\tau_{WR}} \tag{1}$$

$$\frac{\partial \tilde{N}_Q h(z,\tau)}{\partial \tau} = \frac{N_W(1-h)}{\tau_{W2}} - \frac{\tilde{N}_Q h}{\tau_{2W}} - \frac{\tilde{N}_Q h(1-f)}{\tau_{21}} + \frac{\tilde{N}_Q f(1-h)}{\tau_{12}} \tag{2}$$

$$\frac{\partial \tilde{N}_Q f(z,\tau)}{\partial \tau} = \frac{\tilde{N}_Q h(1-f)}{\tau_{21}} - \frac{\tilde{N}_Q f(1-h)}{\tau_{12}} - \frac{\tilde{N}_Q f^2}{\tau_{1R}} - \frac{g}{\hbar\omega_s W(z)} P_s(z,\tau) \tag{3}$$

N_W is the carrier density of the WL, I is the bias current, e is the electron charge, V is the total volume of the active region, f and h represent the electron occupation probability of the GS and ES, respectively, τ_{w2} is the effective capture time into QDs, N_Q is the surface density of QDs, $\tilde{N}_{Q=}N_Q/L_W$ is the effective volume density of QDs where L_w is the effective thickness of the active layer. τ_{2w} is the electron escape time from the ES to the WL and τ_{WR} is the electron spontaneous recombination lifetime of the WL which includes radiative, nonradiative and Auger recombinations. τ_{21} is the electron relaxation time from the ES to the GS, τ_{12} is the electron excitation time from the GS to the ES and τ_{1R} is the spontaneous radiation lifetime in the QD. The gain expression is given by $g=g_{max}(2f-1)$, g_{max} is the maximum modal gain which depends on parameters such as the mean size of QDs, the confinement factor, number of QD layers, and the effective cross-section of the QDs at the signal frequency. P_s is optical power, z is the distance in the longitudinal direction and $\hbar\omega$ is the photon energy. $W(z)$ is the cross-section of the active layer which can be considered through the following relations for the exponential and linear structures, respectively [20].

$$W(z) = W_{in} \exp\left[\frac{z}{L}\ln\left(\frac{W_{out}}{W_{in}}\right)\right] \tag{4}$$

$$W(z) = W_{in} + \left(\frac{W_{out} - W_{in}}{L}\right) z \tag{5}$$

W_{in} and W_{out} are the waveguide input and output widths, respectively and L is the length of the amplifier.

The pulse propagation equation can be expressed as:

$$\frac{\partial P_s(z,\tau)}{\partial z} = (g - \alpha_{\text{int}} - \alpha_{tap}) P_s(z,\tau) \tag{6}$$

$$\alpha_{tap} = -W(z)\frac{d}{dz}\left(\frac{1}{W(z)}\right) \tag{7}$$

where α_{int} is the material loss coefficient or adsorption coefficient of the material in the signal wavelength and α_{tap} is used to describe intensity variation such as focusing and spreading due to the waveguide structure [16]. It should be noted that depending on the direction of light propagation, α_{tap} can act like a gain coefficient or loss coefficient [22]. The unchirped input Gaussian pulse is defined as:

$$P_{in}(\tau) = \frac{E_{in}}{\tau_0\sqrt{\pi}} \exp(-\frac{\tau^2}{\tau_0^2}) \tag{8}$$

where P_{in} is the input optical power and E_{in} is the input pulse energy. $\tau=t-z/v_g$ which t is the actual time and v_g is the group velocity. $\tau_m=1.665\tau_0$ which τ_m is the full width at half maximum (FWHM) of the input pulse and τ_0 is related to pulse width. The rate equations are solved using the 4th order Runge-Kutta numerical method. The cavity length is divided into 200 sections to solve the rate equations. The values of the parameters used in the simulations are given in Table 1.

Table 1
TW-QDSOA parameters and corresponding numerical values used in simulations [21].

Symbol	Description	Value
I	Bias current	30 mA
λ	wavelength	1.55 μm
E_{in}	Input energy	0.5 & 5 pJ
e	Electron charge	1.6×10^{-19} C
g_{max}	Maximum modal gain	14 cm^{-1}
N_Q	Surface density of QDs	1×10^{11} cm^{-2}
L	Length of the amplifier	2 mm
W_{in}	Input width of the active region	2 μm
W_{out}	Output width of the active region	10 & 20 μm
L_W	Effective thickness of the active layer	0.1 μm
α_{int}	Absorption coefficient of the material	3 cm^{-1}
τ_{W2}	Effective capture time	3 ps
τ_{2W}	Characteristic escape time	1 ns
τ_{WR}	Spontaneous recombination time	1 ns
τ_{12}	Escape time from the GS to the ES	1.2 ps
τ_{1R}	Spontaneous radiation lifetime in the QD	0.4 ns
τ_{21}	Electron relaxation time from the ES to the GS	0.2 ps

3. Simulation Results and Discussions

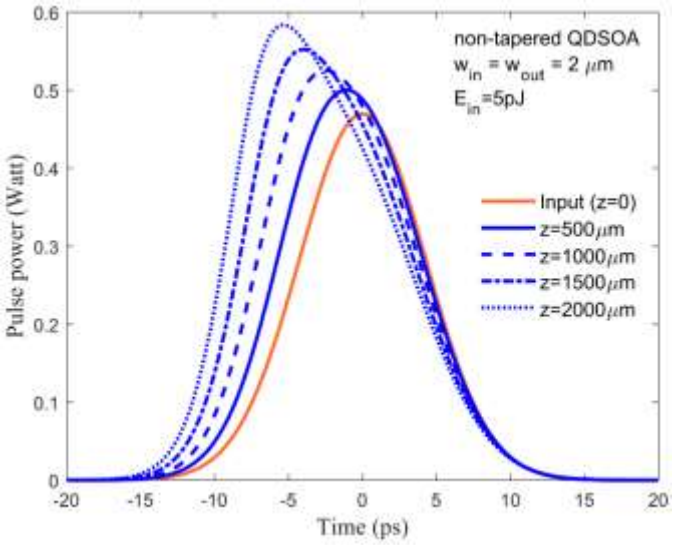

Fig. 2. The amplification of an unchirped input Gaussian pulse inside a non-tapered QDSOA for different cavity lengths (E_{in} =5 pJ).

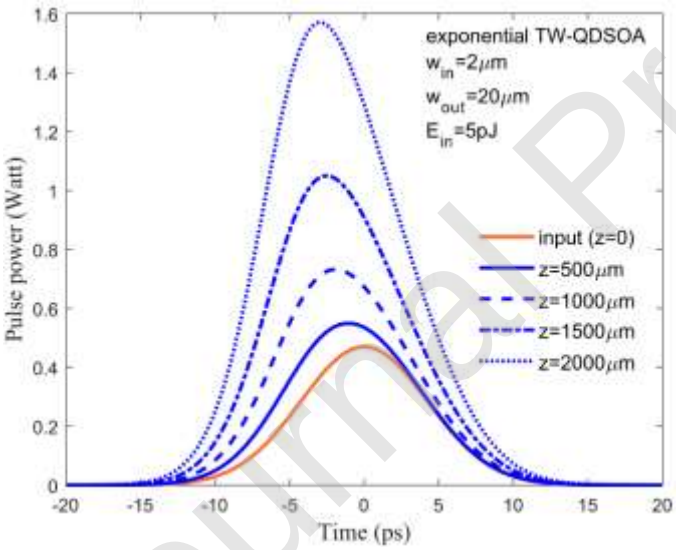

Fig. 3. The amplification of an unchirped Gaussian input pulse inside an exponential TW-QDSOA along the amplifier for different cavity lengths (E_{in} =5 pJ).

In non-tapered QDSOA, the input and output widths of the active region have been assumed to be 2 μm. and the input Gaussian pulsewidth is 10 ps. Fig. 2, depicts the pulse amplification for an unchirped input Gaussian pulse for different cavity lengths along the cavity of a non-tapered QDSOA.

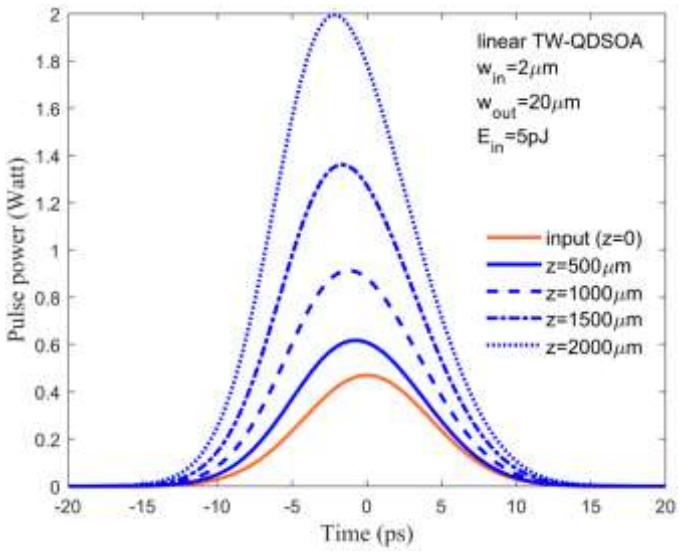

Fig. 4. The amplification of an unchirped Gaussian input pulse inside a linear TW-QDSOA along the amplifier for different cavity lengths (E_{in} =5 pJ).

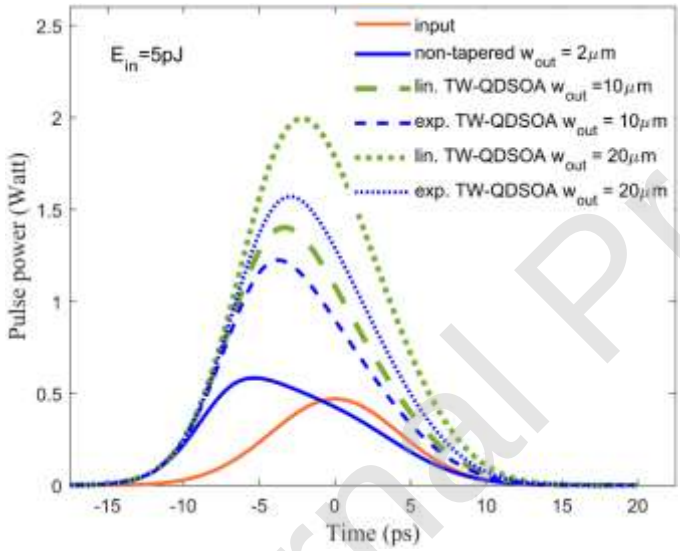

Fig. 5. The amplified output pulse waveforms in non-tapered QDSOA, exponential and linear TW-QDSOA structures with w_{out} =10 and 20 µm (E_{in} =5 pJ).

Figures 3 and 4 illustrate the amplification dynamics of an unchirped Gaussian input pulse for different cavity lengths for exponential and linear TW-QDSOA, respectively. The waveguide widths at the input and output facets of the amplifier are 2 μm and 20 μm for the linear and exponential TW-QDSOAs and the waveguide width increases along the cavity according to equations (4) and (5), respectively. As it is shown in Figs. 3 and 4, the output waveform is asymmetric which is a common feature in optical amplifiers. To explain this phenomenon, it should be considered that the stimulated recombination reduces the carrier density when the power of the optical signal increases and thus, reduces the gain of the amplifier [23]. When a Gaussian pulse propagates inside the cavity, the rising edge causes the amplifier to saturate, therefore, the trailing edge slows down and receives less gain than the rising edge. As a result, the output waveform is distorted and the pulse peak has deviated.

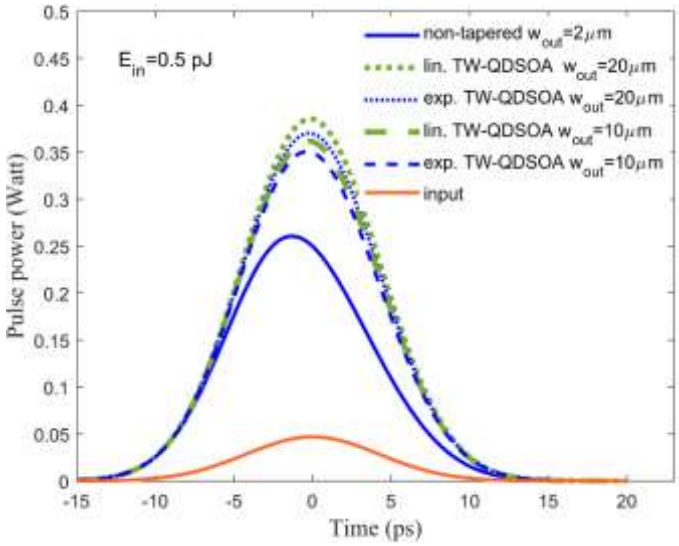

Fig. 6. The amplified output pulse waveforms in non-tapered QDSOA, exponential and linear TW-QDSOA structures with w_{out} =10 and 20 µm (E_{in} =0.5 pJ).

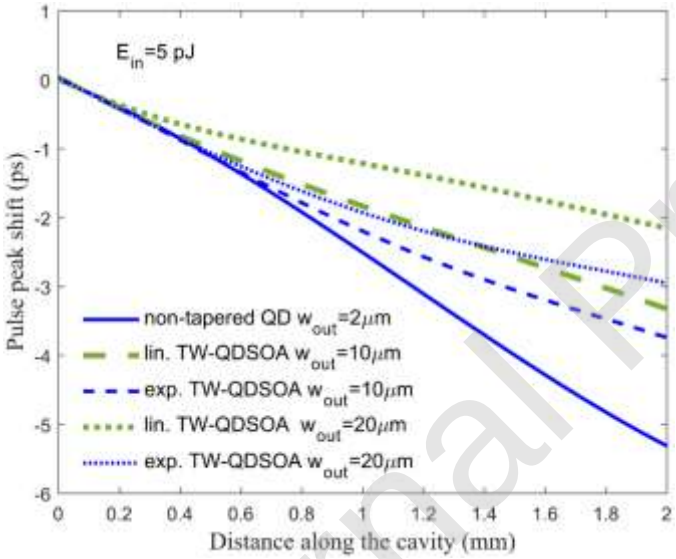

Fig. 7. Shift of pulse peak along the amplifier for non-tapered, linear and exponential TW-QDSOA structures with w_{out} =10 and 20 µm (E_{in} =5 pJ).

In order to have a fair comparison, we have obtained the output waveforms for three structures with w_{out} =10 and 20 μm and E_{in} =5 and 0.5 pJ in Fig. 5 and 6, respectively. As shown in Fig. 5, the pulse amplified by the linear amplifier has less distortion and experiences higher gain compared with the exponential and non-tapered amplifiers since the cross-sectional area of the active region in linear amplifier is larger than the exponential and non-tapered amplifiers. It is also observed that the output waveform amplified by the non-tapered QDSOA is more distorted than other amplifiers. The peak power of the linear amplifier is more than the exponential and non-tapered structures (the peak power values are 2, 1.56, 1.4, 1.22 and 0.58 Watt for linear (w_{out}=20 μm), exponential (w_{out}=20 μm), linear (w_{out}=10 μm), exponential (w_{out}=10 μm) and non-tapered (w_{out} =2 μm), respectively). Due to low input signal energy, the peak power of the amplified signals at the output is less distorted as it is clear from Fig. 6.

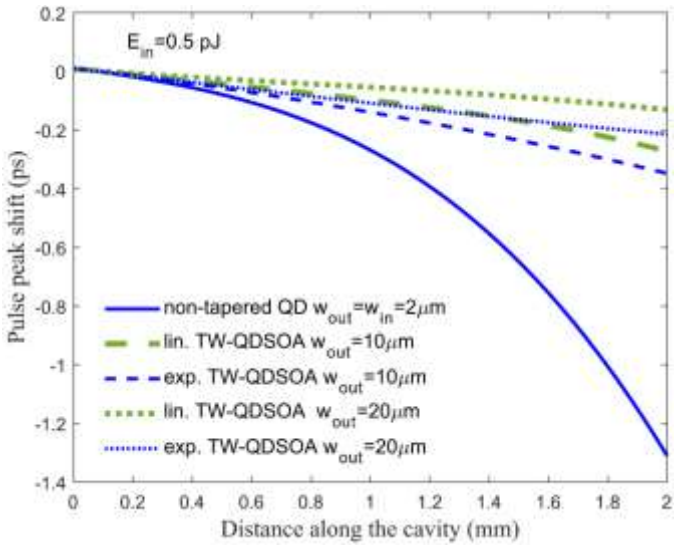

Fig. 8. Shift of pulse peak along the amplifier for non-tapered, linear and exponential TW-QDSOA structures with w_{out} =10 and 20 µm (E_{in} =0.5 pJ).

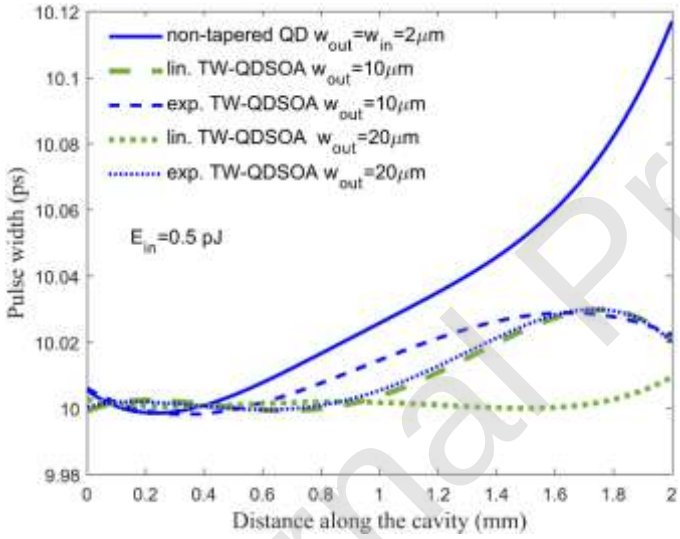

Fig. 9. Variation in pulse width along the amplifier for non-tapered, linear and exponential TW-QDSOA structures with w_{out} =10 and 20 µm (E_{in} =0.5 pJ).

The peak power values of Fig. 6 are 0.38, 0.37, 0.36, 0.35 and 0.25 Watt for linear (w_{out}=20 μm), exponential (w_{out}=20 μm), linear (w_{out}=10 μm), exponential (w_{out}=10 μm) and non-tapered (w_{out} =2 μm) structures, respectively.

Figures 7 and 8 depict the shift of pulse peak along the amplifier for three structures with w_{out} =10 and 20μm with E_{in} =5 and 0.5 pJ, respectively. When the Gaussian pulse propagates along the amplifier, the pulse peak deviates further as the amplifier becomes more saturated as the rising edge experiences more gain. The non-tapered and the linear TW-QDSOA with w_{out} =20 μm have the highest and lowest peak deviations. Also, the larger the active region cross-section, the less saturated the amplifier is and thus, the smaller deviation is obtained. In Fig .7, τ_p =-2.15, -2.92, -3.32, -3.72 and -5.32 ps have been obtained for linear (w_{out}=20 μm), exponential (w_{out}=20 μm), linear (w_{out}=10 μm), exponential (w_{out}=10 μm), and non-tapered (w_{out} =2 μm) structures, respectively.

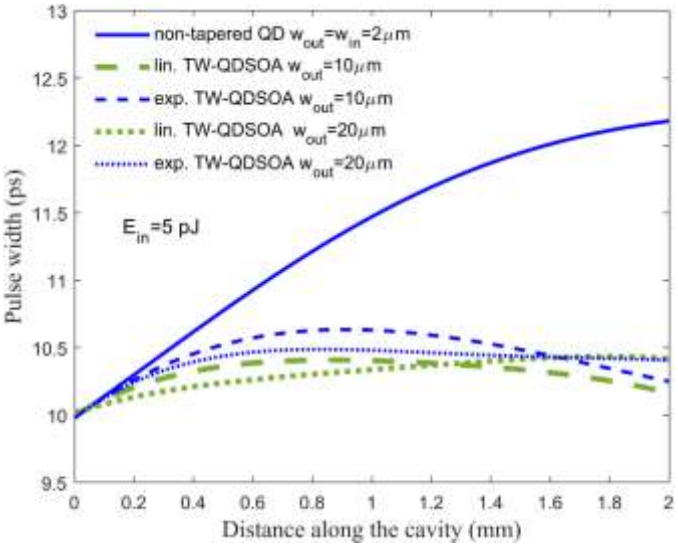

Fig. 10. Variation in pulsewidth along the amplifier for non-tapered, linear and exponential TW-QDSOA structures with w_{out} =10 and 20 µm (E_{in} =5 pJ).

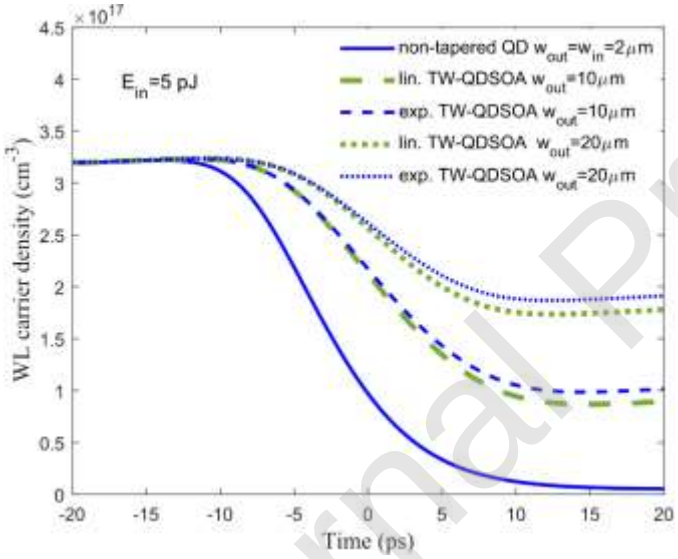

Fig . 11. Carrier density dynamics of the WL for non-tapered, linear and exponential TW-QDSOA structures with w_{out} =10 and 20 µm (E_{in} =5 pJ).

For input signals with low energy, the pulse peak deviation will be lower. As illustrated in Fig. 8, τ_p =-0.12, -0.22, -0.27, -0.35, and -1.3 ps have been obtained for input signal energy of 0.5 pJ in linear (w_{out}=20 μm), exponential (w_{out}=20 μm), linear (w_{out}=10 μm), exponential (w_{out}=10 μm), and non-tapered (w_{out} =2 μm) structures, respectively.

Figures 9 and 10 show the pulse-width variation along the amplifier for three structures with w_{out} =10 and 20 μm and pulse energies of E_{in} =0.5 pJ and E_{in} =5 pJ, respectively. Due to the larger cross-section of the tapered amplifiers and consequently their higher saturation power, pulse-width variations are very small and almost negligible. However, the pulse broadening in the non-tapered amplifier increases with cavity length. As it can be seen in Fig. 9, the pulse-width is almost constant for amplifier lengths smaller than 500 μm because the amplifier is not saturated yet.

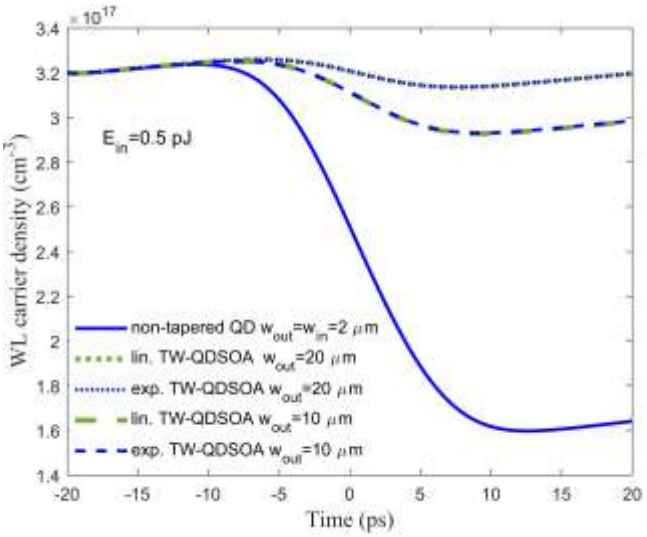

Fig. 12. Carrier density dynamics of the WL for non-tapered, linear and exponential TW-QDSOA structures with w_{out} =10 and 20 µm (E_{in} =0.5 pJ).

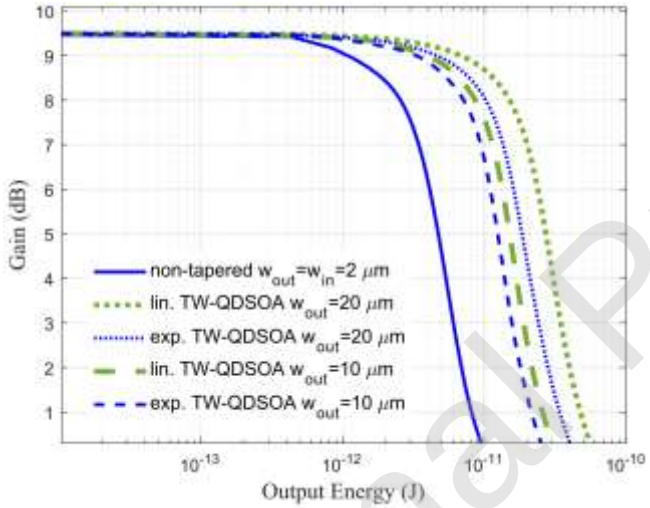

Fig. 13. Variation of pulse energy gain versus output energy in non-tapered QDSOA, exponential and linear TW-QDSOA structures with w_{out} =10 and 20 µm.

As the signal propagates inside the tapered amplifiers, the pulse-width initially increases but then, a pulse compression happens. Signal compression can be associated to the leading edge of the Gaussian pulse which receives higher gain than the trailing edge, therefore, the trailing edge is slightly trimmed. As the amplifier becomes more saturated, the signal compression increases. Therefore, the pulse compression is more considerable in tapered amplifiers. As it can be seen in Fig. 10, pulse widths in tapered amplifier with w_{out}=10 μm is more compressed compared with the tapered amplifier with w_{out}=20 μm.

Figures 11 and 12 display the carrier density dynamics of the WL (N_W) for three structures. As the input signal is amplified along the cavity, N_W decreases since it acts as a reservoir for the GS. As the cross-sectional area of the tapered amplifiers increases, the carrier density reduction is smaller than the non-tapered amplifiers. As shown in Fig .12, the carrier density variation decreases as the input signal energy is decreased to 0.5 pJ.

Figure 13 shows the amplifier gain versus output pulse energy for three structures. As can be seen, the TW-QDSOAs are saturated at higher energies than the non-tapered QDSOA. Since the linear amplifier

waveguide width is larger than the exponential amplifier, the linear amplifier is saturated at higher energies compared with the exponential structure.

4. Conclusion

In this article, we investigated non-tapered, linear and exponential structures for QDSOAs using the numerical calculation of the rate and propagation equations. The waveforms of the amplified output pulses in the three structures were discussed and compared in detail. It was shown that the tapered structures can improve the performance of optical amplifiers. TW-QDSOAs amplify the input signal with lower distortion and higher gain compared to the non-taperd QDSOAs. Also, it was shown that the tapered QDSOAs are saturated at higher powers in comparison with the non-taperd QDSOAs. Results of this research can be generalized to the design of optical wavelength converters and signal-processing plans which utilize QDSOAs as their main processing element.

Declaration of interests

The authors declare that they have no known competing financial interests or personal relationships that could have appeared to influence the work reported in this paper.

References

[1] A. M. de Melo, "Nonlinear applications of semiconductor optical amplifiers for all-optical networks," Citeseer, 2007.

[2] T. Rampone, H.-W. Li, and A. Sharaiha, "Semiconductor optical amplifier used as an in-line detector with the signal DC-component conservation," *Journal of lightwave technology*, vol. 16, p. 1295, 1998.

[3] F. Alimohammadi, R. Yadipour, K. Abbasian, and H. Baghban, "THz-Assisted Instantaneous Gain Switching in Quantum Dot Semiconductor Optical Amplifiers," *IEEE Photonics Technology Letters*, vol. 27, pp. 288-291, 2014.

[4] A. Rostami, H. B. A. Nejad, R. M. Qartavol, and H. R. Saghai, "Tb/s optical logic gates based on quantum-dot semiconductor optical amplifiers," *IEEE Journal of Quantum Electronics*, vol. 46, pp. 354-360, 2010.

[5] M. J. Connelly, *Semiconductor optical amplifiers*: Springer Science & Business Media, 2007.

[6] M. Sugawara, T. Akiyama, N. Hatori, Y. Nakata, H. Ebe, and H. Ishikawa, "Quantum-dot semiconductor optical amplifiers for high-bit-rate signal processing up to 160 Gb s-1 and a new scheme of 3R regenerators," *Measurement Science and Technology*, vol. 13, p. 1683, 2002.

[7] H. Baghban and F. Alimohammadi, "Noise suppression in quantum-dot semiconductor optical amplifiers: A bit rate-SNR analysis," *IEEE Transactions on Electron Devices*, vol. 62, pp. 909-913, 2015.

[8] D. Cotter, R. Manning, K. Blow, A. Ellis, A. Kelly, D. Nesset, *et al.*, "Nonlinear optics for high-speed digital information processing," *Science*, vol. 286, pp. 1523-1528, 1999.

[9] D. Bimberg, M. Grundmann, and N. N. Ledentsov, *Quantum dot heterostructures*: John Wiley & Sons, 1999.

[10] Y. Arakawa and H. Sakaki, "Multidimensional quantum well laser and temperature dependence of its threshold current," *Applied Physics Letters*, vol. 40, pp. 939-941, 1982.

[11] T. Akiyama, M. Ekawa, M. Sugawara, K. Kawaguchi, H. Sudo, A. Kuramata, *et al.*, "An ultrawide-band semiconductor optical amplifier having an extremely high penalty-free output power of 23 dBm achieved with quantum dots," *IEEE Photonics Technology Letters*, vol. 17, pp. 1614-1616, 2005.

[12] M. Sugawara and M. Usami, "Quantum dot devices: Handling the heat," *Nature Photonics*, vol. 3, p. 30, 2009.

[13] S. M. Izadyar, M. Razaghi, and A. Hassanzadeh, "Quantum dot semiconductor optical amplifier: role of second excited state on ultrahigh bit-rate signal processing," *Applied Optics*, vol. 56, pp. 3599-3607, 2017.

[14] P. Borri, W. Langbein, J. M. Hvam, F. Heinrichsdorff, M. H. Mao, and D. Bimberg, "Spectral Hole-Burning and Carrier-Heating Dynamics in Quantum-Dot Amplifiers: Comparison with Bulk Amplifiers," *physica status solidi (b)*, vol. 224, pp. 419-423, 2001.

[15] P. Borri, W. Langbein, J. Hvam, F. Heinrichsdorff, M.-H. Mao, and D. Bimberg, "Ultrafast gain dynamics in InAs-InGaAs quantum-dot amplifiers," *IEEE Photonics Technology Letters*, vol. 12, pp. 594-596, 2000.

[16] G. Bendelli, K. Komori, and S. Arai, "Gain saturation and propagation characteristics of index-guided tapered-waveguide traveling-wave semiconductor laser amplifiers (TTW-SLAs)," *IEEE journal of quantum electronics*, vol. 28, pp. 447-458, 1992.

[17] H. Ghafouri-Shiraz, P. Tan, and T. Aruga, "Analysis of a semi-linear tapered-waveguide laser-diode amplifier," *Microwave and Optical Technology Letters*, vol. 12, pp. 53-56, 1996.

[18] F. Koyama, K.-Y. Liou, A. Dentai, T. Tanbun-Ek, and C. Burrus, "Multiple-quantum-well GaInAs/GaInAsP tapered broad-area amplifiers with monolithically integrated waveguide lens for high-power applications," *IEEE photonics technology letters*, vol. 5, pp. 916-919, 1993.

[19] D. Bossert, J. Marciante, and M. Wright, "Feedback effects in tapered broad-area semiconductor lasers and amplifiers," *IEEE photonics technology letters*, vol. 7, pp. 470-472, 1995.
[20] H. Ghafouri-Shiraz, P. W. Tan, and T. Aruga, "Picosecond pulse amplification in tapered-waveguide laser-diode amplifiers," *IEEE Journal of Selected Topics in Quantum Electronics*, vol. 3, pp. 210-217, 1997.
[21] H. Baghban, R. Ghorbani, and A. Rostami, "Equivalent circuit model of quantum dot semiconductor optical amplifiers: dynamic behaviour and saturation properties," *Journal of Optics A: Pure and Applied Optics*, vol. 11, p. 105205, 2009.
[22] W. Wong and H. Ghafouri-Shiraz, "Dynamic model of tapered semiconductor lasers and amplifiers based on transmission-line laser modeling," *IEEE Journal of selected topics in quantum electronics*, vol. 6, pp. 585-593, 2000.
[23] H. Ghafouri-Shiraz and P. Tan, "Study of a novel laser diode amplifier structure," *Semiconductor science and technology*, vol. 11, p. 1443, 1996.